








Article

Low-Cost Pocket Fluorometer and Chemometric Tools for Green and Rapid Screening of Deoxynivalenol in Durum Wheat Bran

Leonardo Ciaccheri ^{1,*}, Annalisa De Girolamo ^{2,*}, Salvatore Cervellieri ², Vincenzo Lippolis ²,
Andrea Azelio Mencaglia ¹, Michelangelo Pascale ³ and Anna Grazia Mignani ¹

¹ CNR—Istituto di Fisica Applicata “Nello Carrara” (IFAC), Via Madonna del Piano, 10, Sesto Fiorentino, 50019 Florence, Italy; a.mencaglia@ifac.cnr.it (A.A.M.); a.g.mignani@ifac.cnr.it (A.G.M.)

² CNR—Istituto di Scienze delle Produzioni Alimentari (ISPA), Via G. Amendola, 122/O, 70126 Bari, Italy; salvatore.cervellieri@ispa.cnr.it (S.C.); vincenzo.lippolis@ispa.cnr.it (V.L.)

³ CNR—Istituto di Scienze dell’Alimentazione (ISA), Via Roma, 64, 83100 Avellino, Italy; michelangelo.pascale@cnr.it

* Correspondence: l.ciaccheri@ifac.cnr.it (L.C.); annalisa.degirolamo@ispa.cnr.it (A.D.G.)

Abstract: Cereal crops are frequently contaminated by deoxynivalenol (DON), a harmful type of mycotoxin produced by several *Fusarium* species fungi. The early detection of mycotoxin contamination is crucial for ensuring safety and quality of food and feed products, for preventing health risks and for avoiding economic losses because of product rejection or costly mycotoxin removal. A LED-based pocket-size fluorometer is presented that allows a rapid and low-cost screening of DON-contaminated durum wheat bran samples, without using chemicals or product handling. Forty-two samples with DON contamination in the 40–1650 µg/kg range were considered. A chemometric processing of spectroscopic data allowed distinguishing of samples based on their DON content using a cut-off level set at 400 µg/kg DON. Although much lower than the EU limit of 750 µg/kg for wheat bran, this cut-off limit was considered useful whether accepting the sample as safe or implying further inspection by means of more accurate but also more expensive standard analytical techniques. Chemometric data processing using Principal Component Analysis and Quadratic Discriminant Analysis demonstrated a classification rate of 79% in cross-validation. To the best of our knowledge, this is the first time that a pocket-size fluorometer was used for DON screening of wheat bran.

Keywords: deoxynivalenol; DON; wheat bran; fluorescence; chemometrics



Citation: Ciaccheri, L.; De Girolamo, A.; Cervellieri, S.; Lippolis, V.; Mencaglia, A.A.; Pascale, M.; Mignani, A.G. Low-Cost Pocket Fluorometer and Chemometric Tools for Green and Rapid Screening of Deoxynivalenol in Durum Wheat Bran. *Molecules* **2023**, *28*, 7808. <https://doi.org/10.3390/molecules28237808>

Academic Editor: Daniel Cozzolino

Received: 4 October 2023

Revised: 21 November 2023

Accepted: 23 November 2023

Published: 27 November 2023



Copyright: © 2023 by the authors. Licensee MDPI, Basel, Switzerland. This article is an open access article distributed under the terms and conditions of the Creative Commons Attribution (CC BY) license (<https://creativecommons.org/licenses/by/4.0/>).

1. Introduction

Cereals are a nutritious and convenient food option for a balanced diet given the range of health benefits they offer. Indeed, most cereals are a low-fat and a low-calorie source of carbohydrates, are rich in fibers, vitamins, and minerals, and help in lowering the cholesterol level [1–4]. Durum wheat bran for direct human consumption is one of the most added components in high-fiber breakfast cereals, bread and baked goods. It is also assumed as a dietary supplement being rich in magnesium, phosphorus and zinc, helping the immune system; moreover, it has a low glycemic index, thus improving the regulation of blood sugar and preventing spikes in insulin [4,5].

However, cereal crops, such as wheat, maize, barley, oats, and rye, are frequently contaminated by deoxynivalenol (DON), also known as vomitoxin (IUPAC name: 3 α ,7 α ,15-Trihydroxy-12,13-epoxytrichothec-9-en-8-one). DON is a type-B trichothecene mycotoxin, produced as a secondary metabolite of several species of *Fusarium* fungi. Furthermore, levels of DON in wheat bran have been found to be up to three times the levels in unprocessed wheat [6–8]. This contamination represents a significant threat to human health, as the ingestion of DON-contaminated cereals can cause digestive problems, nausea, vomiting, diarrhea, and other abdominal pains. In severe cases, it can also lead to more serious health issues such as anemia, decreased white blood cell count, and impaired immune

function [9–11]. To protect the health of consumers from exposure to DON through the consumption of cereals and cereal-based products, the European Commission has set maximum permitted levels of DON in these food products. In particular, the EU maximum limit for DON in wheat bran intended for direct human consumption has been set at 750 $\mu\text{g}/\text{kg}$ [12].

Conventional analytical methods for determination of DON in cereals mainly imply sample preparation and the use of gas chromatography (GC) with electron-capture or mass spectrometric (MS) detection or liquid chromatography (LC) coupled with UV/DAD or MS detection. Although these methods show high accuracy and precision, they are destructive, expensive, time consuming and unsuitable for screening purposes [13–16]. Factors like promptness and low cost of analysis, minimal sample preparation and environmentally friendly methods are of paramount importance for rapidly responding to the demands of the market. Consequently, in the last decade, other methods have gained wide acceptance such as rapid analytical tools for the screening of DON in cereals. Among them, heterogeneous assays like enzyme-linked immunosorbent assay (ELISA) and lateral flow immunoassay (LFIA), and homogeneous assays like fluorescence polarization immunoassay (FPIA) have been applied to the rapid screening of DON in wheat and derived products, including brans [17–20]. Although these approaches require only minimal sample preparation in terms of homogenization and extraction steps, they are still relatively labor intense, suffer from cross-reactivity of the antibody and require basic laboratory skills and equipment [21]. On the other hand, other approaches based on the use of electronic nose (e-nose) and optical techniques have been proposed as tools for the screening of cereal samples for DON content in a fast and non-destructive way [22–24]. In the last decade, e-nose methods have been proposed to indirectly assess the content of DON in wheat, barley and wheat bran samples by detecting changes in the composition of volatile organic compounds produced by mycotoxigenic fungi during their growth and biochemical processes [25–27]. Moreover, a variety of optical methods has been proposed for the indirect analysis of mycotoxins and fungal contamination in cereals by assessing their appearance and biochemical composition [28–31]. These optical methods include the use of infrared spectroscopy in the near (NIR) and middle (MIR) range and in the visible range with DON as the most targeted mycotoxin in wheat, maize, barley, and oat [32–41]. In some cases, the NIR range was complemented by reflectance measurements in the ultraviolet and visible bands [42–44]. Furthermore, Fourier transform (FT) instrumentation, offering several advantages compared to the traditional dispersive infrared instruments, has been used for the discrimination of DON in wheat and wheat bran [45–49]. NIR spectroscopy has been used more frequently compared to MIR for the prediction of mycotoxins, while imaging techniques like hyperspectral or multispectral imaging have been mainly used for the identification of fungal contamination in cereals. Table 1 summarizes the spectroscopic techniques that have been used to detect the DON contamination in the various types of cereals. The type of detection carried out, whether quantitative or qualitative (i.e., by classes of contamination), is also mentioned.

Fluorescence spectroscopy is another popular method employed in food analyses which has been used in the last decades, enabling the analysis of large-volume data for the identification of sample types and geographical origin of food, as well as for the detection of harmful substances such as mycotoxins and for the quantification of functional components [50–52]. Fujita and co-workers pioneered the use of fluorescence spectroscopy for detecting DON in water solutions using a wavelength range of excitation/emission of 200–340 nm and 500–600 nm, respectively [53,54]. Similarly, with the same scheme of the excitation–emission matrix, Sugiyama et al. (2011) applied fluorescence spectroscopy to wheat samples artificially contaminated with DON [55].

Table 1. Summary of spectroscopic techniques used to detect DON contamination in various types of cereals and the type of detection, whether quantitative or qualitative (i.e., classification based on mycotoxin contamination with respect to a threshold limit).

Spectroscopic Platform	Sample	Detection	Sensitivity	Reference
Near-infrared	Wheat flour	Qualitative	Threshold: 450 µg/kg	[32]
Near-infrared	barley	Qualitative	Threshold: 1250 µg/kg	[33]
Near-infrared	Maize	Quantitative	Limit of detection: 200 µg/kg	[34]
Near-infrared	Whole wheat grain	Quantitative	Limit of detection: 230 µg/kg	[35]
Near-infrared	Wheat kernel	Quantitative	Limit of detection: 400 µg/kg	[37]
Near-infrared	Barley	Quantitative	Limit of detection: 300 µg/kg	[38]
Near-infrared	Ground durum wheat	Qualitative	Threshold: 1400 µg/kg	[45]
Near-infrared	Ground durum wheat	Qualitative	Threshold ≤ 1000 µg/kg 1000 µg/kg < Threshold ≤ 2500 µg/kg Threshold > 2500 µg/kg	[46]
Mid-infrared	Maize	Qualitative	Threshold: 1250 µg/kg	[39]
Mid-infrared	Maize	Qualitative	Threshold: 560 µg/kg	[48]
Infrared	Wheat flour	Quantitative	Limit of detection: 440 µg/kg	[41]
Infrared	Maize	Qualitative	Threshold: 1250 µg/kg	[49]
Near/mid infrared	Wheat bran	Qualitative	Threshold: 400 µg/kg	[47]
Visible/near infrared	Ground oats	Quantitative	Limit of detection: ~200 µg/kg	[44]
UV/visible/near infrared	Maize kernel	Quantitative	Limit of detection: 1500 µg/kg	[42]
UV/visible/near infrared	Ground wheat	Quantitative	Limit of detection: ~200 µg/kg	[43]
Fluorescence	Wheat flour	Quantitative	Limit of detection: ~2.4 mg/kg	[55]

These spectroscopic methods show attractive features such as easy operation, no consumables, affordable cost, rapidity, little or no sample preparation and have the capability for a high sample throughput. Furthermore, as spectroscopy measures the sample as it is, non-destructively, and without any chemicals, solvents, or other treatments, it is considered a “green” analytics tool [56–58]. Indeed, it helps in reducing the environmental impact of food production processes and makes a significant contribution to both sustainable food production and environmental protection efforts [12].

The aim of the present work was to describe a low-cost, non-destructive, “green” and rapid method combined with chemometrics, for the screening of durum wheat bran samples by means of a low-cost pocket-size fluorometer. The cut-off level for DON screening was set at 400 µg/kg DON and was lower than the EU legal limit of 750 µg/kg set for the bran intended for direct human consumption [12]. This value was considered a safety limit, useful to take a decision whether accepting the sample as safe or carrying out a further inspection by means of more accurate but also more expensive standard analytical techniques. So far, to the best of our knowledge, there has been no literature reporting DON detection by means of a low-cost pocket-size fluorometer like the device shown in this paper.

2. Results and Discussion

The DON level in durum wheat bran ranged from ≤40 µg/kg (limit of quantification of the HPLC confirmatory method) to 1650 µg/kg, as shown in Figure 1. Most samples (62%) were naturally contaminated with DON at levels lesser than the EU limit for wheat bran (750 µg/kg). These samples were grouped into two classes: 18 samples had a DON concentration equal to or lower than 400 µg/kg (Class A), while 24 samples had a DON concentration higher than 400 µg/kg (Class B).

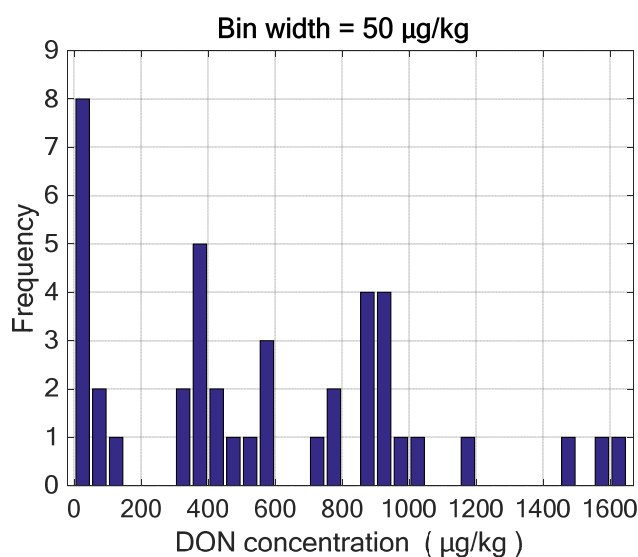


Figure 1. Distribution of DON content in the forty-two durum wheat bran samples as determined by the confirmatory method.

As an example, Figure 2 shows the average fluorescence spectra of wheat bran samples belonging to Classes A and B, excited at the three available wavelengths. An analysis of variance (ANOVA) was carried out at each wavelength to check the significance of difference between the two class means. The *p*-value, offering the probability that the difference between means is due to chance, was calculated. Figure 3 shows the *p*-value as a function of emission wavelength for each excitation wavelength. Significance threshold at a 5% level, which is commonly considered acceptable, as well as the 1% level threshold are also drawn in the plot. For each excitation wavelength, Table 2 summarizes the emission bands where the *p*-value is below a 1% or a 5% significance level threshold.

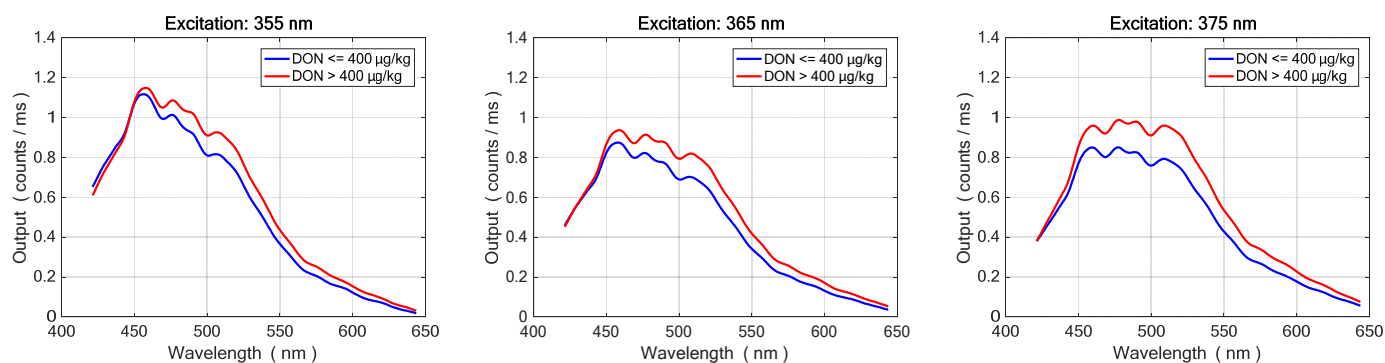


Figure 2. Examples of fluorescence spectra of DON-contaminated wheat bran samples belonging to Class A ($\leq 400 \mu\text{g}/\text{kg}$, blue line) or to Class B ($>400 \mu\text{g}/\text{kg}$, red line), excited at 355 nm (left), 365 nm (center), and 375 nm (right).

Table 2. Emission bands where the *p*-value is below a 1% or a 5% significance level threshold.

Excitation Wavelength	Significance at 5%	Significance at 1%
355 nm	above 517 nm	above 538 nm
365 nm	above 506 nm	532–619 nm
375 nm	above 478 nm	504–634 nm

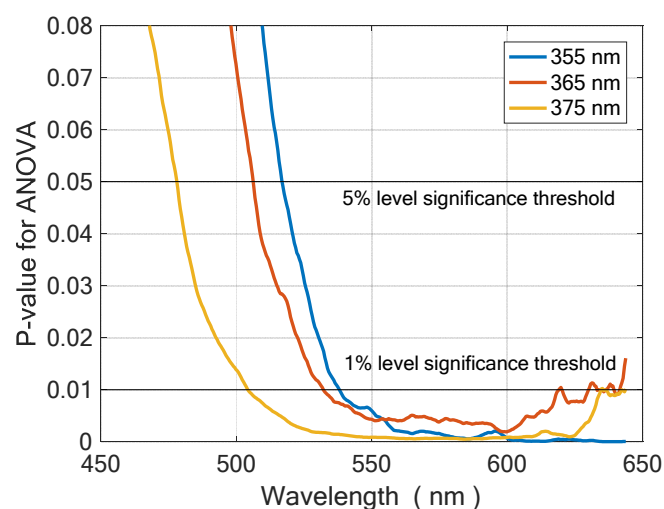


Figure 3. *p*-value of ANOVA as a function of emission wavelength for each excitation wavelength.

Although DON is not fluorescent [59], the occurrence of *Fusarium* fungi in the contaminated wheat bran slightly modified the fluorescence spectra of wheat by inducing different spectral shapes depending on the excitation wavelengths [60]. These effects were more than enough to clearly identify the two classes of contamination sought by using chemometric data processing. Figure 4 shows the Principal Component Analysis (PCA) score plots of training samples for the three excitation wavelengths. It is evident that each wavelength, taken alone, is only partially selective. Data fusion, however, combining information from all three models, achieved a better classification rate. All retained principal components were then merged into a predictor matrix that was fed into the classifier. For all wavelengths, two components were sufficient to explain 99% of total variance. This produced a total of six predictors, which were auto scaled (divided by their standard deviation) for assigning them equal *a priori* importance.

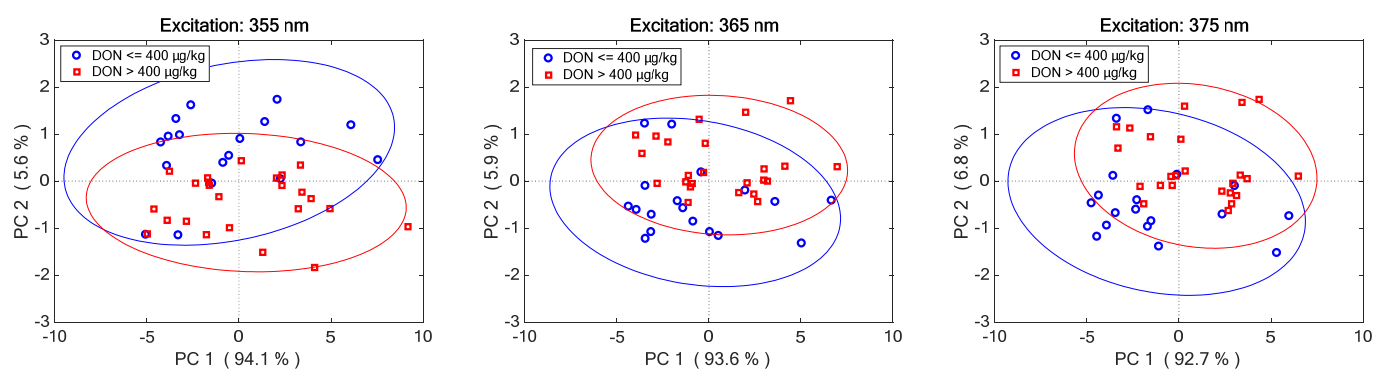


Figure 4. PCA score plots of training samples for the three excitation wavelengths (Ellipses represent 95% confidence limit of each class).

Table 3 summarizes the classification statistics for training and cross-validation, respectively, when considering a single excitation wavelength or combining the data of two or three excitation wavelengths. As described in Section 3.6, models were rated in terms of accuracy, sensitivity, and specificity. Accuracy is the overall classification rate, sensitivity is the true positive rate, and specificity is the true negative rate. The best single-wavelength models were those at 355 nm and 375 nm.

Table 3. Performance parameters (accuracy, sensitivity, and specificity) of the quadratic discriminant analysis for both training and cross-validation, for the different excitation wavelengths and their data fusion. A cut-off of 400 $\mu\text{g}/\text{kg}$ DON was used to distinguish the two classes of DON-contaminated wheat bran samples.

Wavelength (nm)	Training			Cross-Validation		
	Accuracy	Sensitivity	Specificity	Accuracy	Sensitivity	Specificity
355	81%	83%	78%	74%	75%	72%
365	71%	71%	72%	69%	67%	72%
375	74%	75%	72%	74%	75%	72%
355 + 365	83%	83%	83%	76%	75%	78%
365 + 375	86%	88%	83%	79%	83%	72%
355 + 375	86%	88%	83%	79%	75%	83%
355 + 365 + 375	88%	88%	89%	74%	71%	78%

For each pair of excitation wavelengths, we calculated the correlations between the corresponding principal components. The components of the 365 nm model showed very strong correlation with those of both the 355 nm (PC1: 0.97, PC2: -0.97) and 375 nm (PC1: 0.97, PC2: -0.98) models. Instead, the components of 355 nm and 375 nm models showed weaker correlation (PC1: 0.91, PC2: -0.92). In fact, the 355 nm and 375 nm models excited with different efficiency the two fluorescent bands at 450 nm and 530 nm, as shown in Figure 2.

The best two-wavelength model was achieved combining 355 nm and 375 nm, providing a 79% accuracy, a 75% sensitivity, and an 83% specificity in cross-validation. The three-wavelength configuration provided better results in training, but lower statistics in cross-validation, which are a 74% accuracy, a 71% sensitivity, and a 78% specificity in cross-validation. Clearly, adding 365 nm data increased collinearity in the model and introduced some overfitting. Figure 5 shows the plot of membership scores for the two best models. The probability for the lower class is measured along the x -axis, while that of the higher class is measured along the y -axis. The bisector of the first and second quadrant is the decision border.

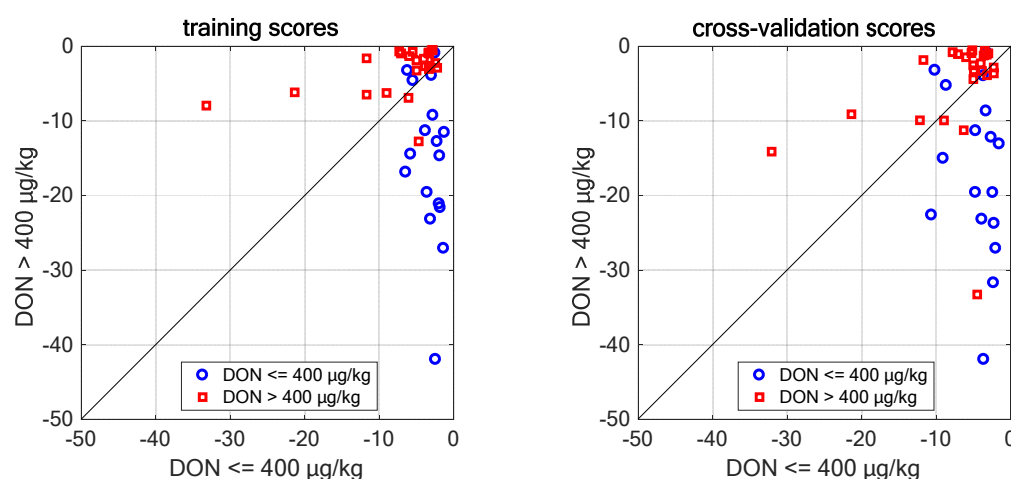


Figure 5. Quadratic Discriminant Analysis score plots for both training (left) and cross-validation (right) of the 355 nm + 375 nm model for classifying wheat bran samples contaminated with DON using intermediate-level data fusion.

For comparison with previous studies that reported the use of fluorescence spectroscopy for DON detection, we note that in those cases, the DON concentration was

much higher, and that bulky and expensive bench-type fluorometers were used, having a wide excitation/emission matrix of 200–340 nm and 500–600 nm, respectively [53–55]. In particular, DON in water solution was measured from the 4×10^3 $\mu\text{g}/\text{kg}$ to 1×10^6 $\mu\text{g}/\text{kg}$ [53], while DON in artificially spiked samples was measured from 2.4×10^2 $\mu\text{g}/\text{kg}$ to 26×10^3 $\mu\text{g}/\text{kg}$ [54,55].

3. Materials and Methods

3.1. Reagents and Apparatus

Acetonitrile of an HPLC grade was bought from Mallinckrodt Baker (Milan, Italy); ultrapure water was produced by a Millipore Milli-Q system (Millipore, Bedford, MA, USA). Deoxynivalenol (DON) standard was purchased from Sigma-Aldrich (Milan, Italy), while DON immunoaffinity columns (DONtest™ HPLC) were from Vicam, a Waters Business (Milford, MA, USA). Glass microfiber (Whatman GF/A) and paper filters (Whatman No. 4) were bought from Whatman (Maidstone, UK).

3.2. Durum Wheat Bran Samples

Forty-two samples (300 g each) of naturally contaminated durum wheat bran samples were collected from a local Italian mill farming. Each sample was finely ground by Tecator Cyclotec 1093 (International PBI, Hoganas, Sweden) laboratory mill equipped with a 500 μm sieve, leading to a homogeneous sample with a fine particle size. Then, samples were manually homogenized and stored at +5 °C until HPLC analysis and fluorescence measurements.

3.3. Wheat Bran Sample Analysis by Reference Method

Milled durum wheat bran samples were analyzed by HPLC for the quantitative determination of DON to be used for the development of the fluorometric method. Each sample was analyzed according to the procedure described by De Girolamo et al. 2019 [47]. Briefly, 12.5 g of the ground sample were extracted by blending for 2 min with 100 mL of phosphate buffer solution (PBS, 10 mM sodium phosphate, 0.85% sodium chloride, pH = 7.4). Then, the extract was filtered through filter paper (Whatman No. 4) and then by glass microfiber filter (Whatman GF/A). Then, an aliquot of 2 mL of the filtered extract was cleaned up through the DONtest™ immunoaffinity column, and after washing the column by passing 5 mL of water through it, DON was recovered by elution with 1.5 mL of methanol. The eluate was dried under air stream at 50° C, redissolved into 0.25 mL of the mobile phase (acetonitrile/water, 8:92; v/v) and an aliquot of 0.05 mL was analyzed by LC (Agilent 1100 Series, Agilent Technology, Palo Alto, CA, USA) with the diode array detector set at 220 nm.

The DON levels in the 42 wheat bran samples ranged from ≥ 40 $\mu\text{g}/\text{kg}$ (quantification limit of the HPLC method) to 1650 $\mu\text{g}/\text{kg}$.

3.4. Fluorometer Assembly

The low-cost fluorometer built for this experiment was a pocket-size device that utilized an LED array for illumination and a miniaturized spectrometer for detection. The hardware module was operated by a laptop PC via a customized Labview® software (Version 18.0.1f4) interface (National Instruments Corp., Austin, TX, USA). Figure 6 shows a rendering of the fluorometer. The optical head providing the fluorescence excitation was made of a housing for twelve circularly arranged LEDs. They were positioned at a 45° angle with respect to the axis of detection, which was in the center of the circle. Three wavelengths were considered for fluorescence excitation, i.e., 355 nm, 365 nm, and 375 nm. Four identical sets of these three LEDs were sequentially placed in circular array housing. They were powered by means of a commercially available electronic controller (PhidgetsLED1031, Phidgets Inc., Calgary, AB, Canada), which was USB-connected to a laptop PC. The optical head was butt-coupled to a cylinder housing the detector, which was an Ocean ST-visible microspectrometer (Ocean Insight, Duiven, The Netherlands) operating in the 350–810 nm

range, having a 1.5 nm spectroscopic resolution. Because the LED spectrum extends in the visible range, a short-pass filter blocking illumination wavelengths longer than 400 nm was inserted between the optical head and the measurement spot. This filter had a small hole in correspondence of the spectrometer input slit to allow the detection of the backscattered fluorescence light intensity at wavelengths longer than 400 nm.

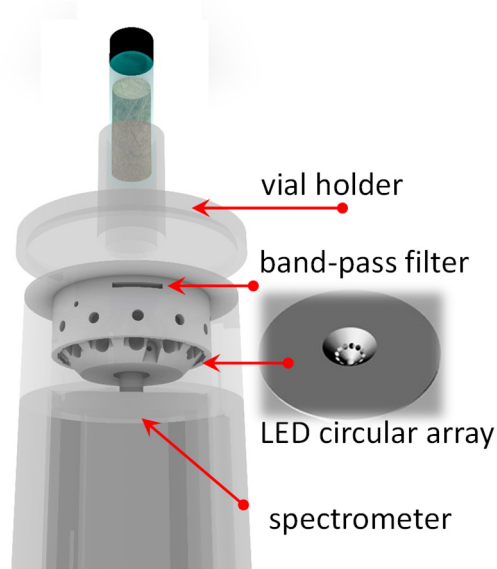


Figure 6. Rendering of the fluorimeter.

The three excitation wavelengths were operated in sequence (four LEDs at the same wavelength at a time), and the emitted fluorescence spectra were recorded synchronously with each excitation wavelength. Spectra acquisition was achieved using the USB port of the spectrometer, connected to the laptop. In practice, this scheme allowed us obtention of a low-cost, pocket-size, and versatile device providing a configuration similar to a three-wavelength scanning fluorescence spectroscopy.

A custom Labview[®] (Version 18.0.1f4) interface was programmed for operating LEDs, spectrometer, detector acquisition, and the sequence of measurements. The software controlled the LED current, the acquisition from the spectrometer, and displayed the measured spectra that could be saved as an Excel file. Depending on the wavelengths, LEDs were powered with different currents for equalizing the light intensity used for fluorescence excitation. The custom software operating the fluorimeter was programmed to acquire the “dark” background spectrum, according to the selected integration times, and to subtract it from the sample fluorescence spectrum.

The casing that housed all optoelectronic components was lightweight and handy. It was 3D printed (KLONER3D[®]240, KLONER3D[®], Firenze, Italy) using a polylactic acid wire. A vial holder was also 3D printed to suitably position the bran sample in front of the illumination/detection optics. The practical implementation of the fluorimeter including the vial holder is shown in Figure 7.

3.5. Wheat Bran Sample Analysis by Fluorescence

For each sample, an aliquot of 1.6 g wheat bran was transferred in a 4 mL glass vial sealed with a safety cap that was allocated in the vial holder and analyzed by the fluorimeter. The fluorescence spectra of all bran samples, excited by the three wavelengths, were acquired by scanning 4 times each sample. The time analysis was approximately 13 s for all wavelengths.



Figure 7. The fluorometer (center), with the supply unit (left) and with the vial holder (right).

3.6. Multivariate Statistical Analysis

Spectra processing and multivariate data analysis was carried out in MATLAB[®] R2016b (MathWorks, Natick, MA, USA) using custom-made subroutines. For each sample, the average spectrum of the 4 scans obtained at each of the three wavelengths was used for data processing. Before development and validation of chemometric models, the fluorometric spectral data were preprocessed to reduce the spectral baseline shift and noise. A two-stage smoothing was applied to each spectrum. First, a 3 pts median filter was used for removing narrow noise spikes; then, a boxcar average filter with a 21 pts window (about 10 nm wide) was used for refined smoothing. Minimum subtraction was applied for removing the effect of random background fluctuations. As previously reported by De Girolamo et al. 2019 [47], a cut-off value of 400 $\mu\text{g}/\text{kg}$ that was below the EC ML for DON in wheat bran (i.e., 750 $\mu\text{g}/\text{kg}$) [12] was used to discriminate wheat bran samples into two classes, A and B. Based on their DON content measured by HPLC analysis, samples were considered as compliant when $[\text{DON}] \leq 400 \mu\text{g}/\text{kg}$ (class A) and not compliant when $[\text{DON}] > 400 \mu\text{g}/\text{kg}$ (class B). Using this screening approach, only samples classified as not compliant should be re-analyzed by the confirmatory method, thus reducing the total number of analyses.

The Leave-One-Out (LOO) cross-validation was used for evaluating the classification performance given the limited number of available samples.

Intermediate-level data fusion was employed for combining information coming from different excitation wavelengths. Spectral information was first compressed, for each excitation wavelength, by means of Principal Component Analysis (PCA) [61]. Then, significant principal components coming from all models were merged into a predictor matrix. Data fusion at PCA level allows reduction in the level of noise introduced in the model, because only structural information from each source is retained [62,63].

In each PCA model, two principal components explained 99% of total variance, offering a total of six predictors. Quadratic Discriminant Analysis (QDA) classification was applied to the joint predictor matrix for sample classification. Like Linear Discriminant Analysis (LDA), QDA assumes that all classes are distributed according to multivariate Gaussian distribution, but it does not assume all classes have the same within-class variance. It is, therefore, more flexible [64]. QDA assigned two scores to each sample depending on its position in the predictor space and proportional to the logarithm of class membership probabilities. Consequently, each sample was assigned to its most probable class. Test samples were projected onto each PCA model and then classified in the same way. Classification rates and confusion matrices were calculated for both training and test set for evaluating classifier performance.

By assuming that Class A is that of non-compliant samples, samples were defined as true positive (TP) if they were correctly classified as A or false negative (FN) if they

are classified as belonging to Class B. Similarly, samples of Class B considered compliant were defined as true negative (TN) if they were correctly found as belonging to Class B or false positive (FP) if they were classified as Class A. QDA performances on each set were assessed in terms of accuracy, sensitivity, and specificity according to the confusion matrices for binary classification [65,66] by using the following formulas:

$$\text{Sensitivity} = [\text{TP}/(\text{TP} + \text{FN})] \times 100, \quad (1)$$

$$\text{Specificity} = [\text{TN}/(\text{TN} + \text{FP})] \times 100, \quad (2)$$

$$\text{Accuracy} = [(\text{TP} + \text{TN})/(\text{TP} + \text{TN} + \text{FP} + \text{FN})] \times 100, \quad (3)$$

where

- sensitivity is defined as the fraction of samples belonging to Class A, correctly classified by the model and is a measure of the confidence level of the class space;
- specificity is defined as the fraction of samples not belonging to Class A that are correctly rejected by the model;
- accuracy is defined as the fraction of correctly classified samples with respect to the entire set.

4. Conclusions and Future Perspectives

An LED-based pocket-size fluorometer was developed in combination with chemometrics for green and rapid screening of DON in durum wheat bran samples. A cut-off limit of 400 µg/kg was set as a threshold useful to make a decision of whether to accept the sample as compliant with respect to the EU ML for DON in wheat bran or to carry out a further analysis by a more expensive standard analytical technique.

By considering all excitation wavelengths, we spotted the wavelength combinations providing the best classification rates. The chemometric approach using intermediate-level data fusion (PCA + QDA) achieved classification rates in the 74–79% range in cross-validation, 355 nm + 375 nm being the best wavelength combination.

To the best of our knowledge, this is the first time that fluorescence spectroscopy carried out by means of a pocket-size fluorometer was successfully used for screening wheat bran naturally contaminated by DON with a contamination threshold of 400 µg/kg. Further activities will focus on making the fluorometer fully standalone by replacing the laptop PC currently used by means of a suitably programmed data processing unit and display. In addition, a new design of the cone-shaped optical head ending in a glass window is underway, so that the bran sample can be measured directly without using a vial for high-throughput screening. The ultimate objective is to transform this device into a high-throughput analytical platform that is cost effective for small mills. This pocket-size device will facilitate a rapid and non-destructive assessment of DON contamination onset during storage and pre-packaging stages without the need for chemicals or specialized by personnel, consequently ensuring the safety of the product before it enters the food chain.

Author Contributions: L.C., A.D.G., M.P. and A.G.M. conceived the experiment, A.D.G. and M.P. provided the wheat samples, L.C. and A.G.M. performed the spectroscopic measurements, L.C. performed the chemometric data processing, A.D.G., S.C. and V.L. performed the HPLC measurements and provided the reference data, A.A.M. designed and built the fluorometer and the software interface. All authors equally contributed to the preparation, writing, and editing of the manuscript. All authors have read and agreed to the published version of the manuscript.

Funding: This research was partially funded by the Italian Ministry of Education, University and Research, project No. CTN01 00230CL.A.N. Cluster Tecnologici Nazionali—SAFE&SMART “New enabling technologies for food safety and food chain integrity within a global scenario”.

Institutional Review Board Statement: Not applicable.

Informed Consent Statement: Not applicable.

Data Availability Statement: Data are contained within the article.

Conflicts of Interest: The authors declare no conflict of interest.

References

1. Garutti, M.; Nevola, G.; Mazzeo, R.; Cucciniello, L.; Totaro, F.; Bertuzzi, C.A.; Caccialanza, R.; Pedrazzoli, P.; Puglisi, F. The impact of cereal grain composition on the health and disease outcomes. *Front. Nutr.* **2022**, *9*, 888974. [[CrossRef](#)]
2. Garg, M.; Sharma, A.; Vats, S.; Tiwari, V.; Kumari, A.; Mishra, V.; Krishania, M. Vitamins in Cereals: A critical review of content, health effects, processing losses, bioaccessibility, fortification, and biofortification strategies for their improvement. *Front. Nutr.* **2021**, *8*, 586815. [[CrossRef](#)] [[PubMed](#)]
3. Polonskiy, V.; Loskutov, I.; Sumina, A. Biological role and health benefits of antioxidant compounds in cereals. *Biol. Commun.* **2020**, *65*, 53–67. [[CrossRef](#)]
4. Borneo, R.; León, A.E. Whole grain cereals: Functional components and health benefits. *Food Funct.* **2012**, *3*, 110–119. [[CrossRef](#)]
5. Williams, P.G. The benefits of breakfast cereal consumption: A systematic review of the evidence base. *Adv. Nutr.* **2014**, *5*, 636S–673S. [[CrossRef](#)] [[PubMed](#)]
6. Tibola, C.S.; Fernandes, J.M.C.; Guarienti, E.M.; Nicolau, M. Distribution of Fusarium mycotoxins in wheat milling process. *Food Control* **2015**, *53*, 91–95. [[CrossRef](#)]
7. Visconti, A.; Haidukowski, M.; Pascale, M. Reduction of deoxynivalenol during durum wheat processing and spaghetti cooking. *Toxicol. Lett.* **2004**, *153*, 181–189. [[CrossRef](#)]
8. Kushiro, M. Effects of milling and cooking processes on the deoxynivalenol content in wheat. *Int. J. Mol. Sci.* **2008**, *9*, 2127–2145. [[CrossRef](#)]
9. Sobrova, P.; Adam, V.; Vasatkova, A.; Beklova, M.; Zeman, L.; Kizek, R. Deoxynivalenol and its toxicity. *Interdiscip. Toxicol.* **2010**, *3*, 94–99. [[CrossRef](#)]
10. Pestka, J.J. Deoxynivalenol: Mechanisms of action, human exposure, and toxicological relevance. *Arch. Toxicol.* **2010**, *84*, 663–679. [[CrossRef](#)]
11. European Food Safety Authority. EFSA Panel on Contaminants in the Food Chain (CONTAM). *EFSA J.* **2017**, *15*, 4718.
12. European Union. Commission Regulation (EC) No. 1126/2007 of 28 September 2007 (amending Regulation No. 1881/2006 of 19 December 2006) setting maximum levels for certain contaminants in foodstuffs as regards Fusarium toxins in maize and maize products. *Off. J. Eur. Union* **2007**, *L255*, 14–17.
13. Janik, E.; Niemcewicz, M.; Podogrocki, M.; Ceremuga, M.; Gorniak, L.; Stela, M.; Bijak, M. The existing methods and novel approaches in mycotoxins' detection. *Molecules* **2021**, *26*, 3981. [[CrossRef](#)]
14. Turner, N.W.; Subrahmanyam, S.; Piletsky, S.A. Analytical methods for determination of mycotoxins: A review. *Anal. Chim. Acta* **2009**, *632*, 168–180. [[CrossRef](#)] [[PubMed](#)]
15. Pereira, V.L.; Fernandes, J.O.; Cunha, S.C. Mycotoxins in cereals and related foodstuffs: A review on occurrence and recent methods of analysis. *Trends Food Sci. Technol.* **2014**, *36*, 96–136. [[CrossRef](#)]
16. Astoreca, A.; Ortega, L.; Fígoli, C.; Cardós, M.; Cavaglieri, L.; Bosch, A.; Alconada, T. Analytical techniques for deoxynivalenol detection and quantification in wheat destined for the manufacture of commercial products. *World Mycotoxin J.* **2016**, *10*, 111–120. [[CrossRef](#)]
17. Zhou, S.; Xu, L.; Kuang, H.; Xiao, J.; Xu, C. Immunoassays for rapid mycotoxin detection: State of the art. *Analyst* **2020**, *145*, 7088–7102. [[CrossRef](#)]
18. Lippolis, V.; Pascale, M.; Visconti, A. Optimization of a fluorescence polarization immunoassay for rapid quantification of deoxynivalenol in durum wheat-based products. *J. Food Prot.* **2006**, *69*, 2712–2719. [[CrossRef](#)]
19. Valenzano, S.; Lippolis, V.; Pascale, M.; De Marco, A.; Maragos, C.M.; Suman, M.; Visconti, A. Determination of deoxynivalenol in wheat bran and whole-wheat flour by fluorescence polarization immunoassay. *Food Anal. Methods* **2014**, *7*, 806–813. [[CrossRef](#)]
20. Agriopoulou, S.; Stamatelopoulou, E.; Varzakas, T. Advances in analysis and detection of major mycotoxins in foods. *Foods* **2020**, *9*, 518. [[CrossRef](#)]
21. Bueno, D.; Istamboulie, G.; Muñoz, R.; Marty, J.L. Determination of mycotoxins in food: A review of bioanalytical to analytical methods. *Appl. Spectrosc. Rev.* **2015**, *50*, 728–774. [[CrossRef](#)]
22. Cheli, F.; Ottoboni, M.; Fumagalli, F.; Mazzoleni, S.; Ferrari, L.; Pinotti, L. E-nose technology for mycotoxin detection in feed: Ready for a real context in field application or still an emerging technology? *Toxins* **2023**, *15*, 146. [[CrossRef](#)] [[PubMed](#)]
23. Saccon, F.A.M.; Parcey, D.; Paliwal, J.; Sherif, S.S. Assessment of Fusarium and deoxynivalenol using optical methods. *Food Bioprocess Technol.* **2017**, *10*, 34–50. [[CrossRef](#)]
24. Zareef, M.; Arslan, M.; Hassan, M.M.; Ahmad, W.; Ali, S.; Li, H.; Ouyang, Q.; Wu, X.; Hashim, M.M.; Chen, Q. Recent advances in assessing qualitative and quantitative aspects of cereals using nondestructive techniques. *Trends Food Sci. Tech.* **2021**, *116*, 815–828. [[CrossRef](#)]
25. Lippolis, V.; Pascale, M.; Cervellieri, S.; Damascelli, A.; Visconti, A. Screening of deoxynivalenol contamination in durum wheat by MOS-based electronic nose and identification of the relevant pattern of volatile compounds. *Food Control* **2014**, *37*, 263–271. [[CrossRef](#)]

26. Lippolis, V.; Cervellieri, S.; Damascelli, A.; Pascale, M.; Di Gioia, A.; Longobardi, F.; De Girolamo, A. Rapid prediction of deoxynivalenol contamination in wheat bran by MOS-based electronic nose and characterization of the relevant pattern of volatile compounds. *J. Sci. Food Agric.* **2018**, *98*, 4955–4962. [[CrossRef](#)]
27. Camardo Leggieri, M.; Mazzoni, M.; Bertuzzi, T.; Moschini, M.; Prandini, A.; Battilani, P. Electronic nose for the rapid detection of deoxynivalenol in wheat using classification and regression trees. *Toxins* **2022**, *14*, 617. [[CrossRef](#)]
28. Levasseur-Garcia, C. Updated overview of infrared spectroscopy methods for detecting mycotoxins on cereals (corn, wheat, and barley). *Toxins* **2018**, *10*, 38. [[CrossRef](#)]
29. Freitag, S.; Sulyok, M.; Logan, N.; Elliott, C.T.; Krska, R. The potential and applicability of infrared spectroscopic methods for the rapid screening and routine analysis of mycotoxins in food crops. *Compr. Rev. Food Sci. Food Saf.* **2022**, *6*, 5199–5224. [[CrossRef](#)]
30. Bilal, M.; Xiaobo, Z.; Arslan, M.; Tahir, H.E.; Li, Z.; Shi, J.; Usman, M. Nondestructive spectroscopic techniques for detection of fungal and mycotoxin infections in food products: A review. *Spectroscopy* **2020**, *35*, 28–36.
31. Zhang, S.; Liu, S.; Shen, L.; Chen, S.; He, L.; Liu, A. Application of near-infrared spectroscopy for the nondestructive analysis of wheat flour: A review. *Curr. Res. Food Sci.* **2022**, *5*, 1305–1312. [[CrossRef](#)]
32. Tyska, D.; Mallmann, A.; Gressler, L.T.; Mallmann, C.A. Near-infrared spectroscopy as a tool for rapid screening of deoxynivalenol in wheat flour and its applicability in the industry. *Food Addit. Contam. Part A* **2021**, *38*, 1958–1968. [[CrossRef](#)] [[PubMed](#)]
33. Dos Santos Caramês, E.T.; Peacetime, K.C.; Alves, L.T.; Lima-Pallone, J.A.; de Oliveira Rocha, L. NIR spectroscopy and chemometric tools to identify high content of deoxynivalenol in barley. *Food Addit. Contam. Part A* **2020**, *37*, 1542–1552. [[CrossRef](#)] [[PubMed](#)]
34. Miedaner, T.; Han, S.; Kessel, B.; Ouzunova, M.; Schrag, T.; Urx, F.H.; Melchinger, A.E. Prediction of deoxynivalenol and zeralenone concentration in *Fusarium graminearum* inoculated backcross populations of maize by symptom rating and near-infrared spectroscopy. *Plant Breed.* **2015**, *134*, 529–534. [[CrossRef](#)]
35. Dvořáček, V.; Prohasková, A.; Chrpová, J.; Štočková, L. Near infrared spectroscopy for deoxynivalenol content estimation in intact wheat grain. *Plant Soil Environ.* **2012**, *58*, 196–203. [[CrossRef](#)]
36. Peiris, K.H.S.; Pumphrey, M.O.; Dowell, F.E. NIR absorbance characteristics of deoxynivalenol and of sound and *Fusarium*-damaged wheat kernels. *J. Near Infrared Spectrosc.* **2009**, *17*, 213–221. [[CrossRef](#)]
37. Pettersson, H.; Åberg, L. Near infrared spectroscopy for determination of mycotoxins in cereals. *Food Control* **2003**, *14*, 229–232. [[CrossRef](#)]
38. Ruan, R.; Li, Y.; Lin, X.; Chen, P. Non-destructive determination of Deoxynivalenol levels in barley using near-infrared spectroscopy. *Appl. Eng. Agric.* **2002**, *18*, 549–553. [[CrossRef](#)]
39. Sieger, M.; Kos, G.; Sulyok, M.; Godejohann, M.; Krska, M.; Mizaikoff, B. Portable infrared laser spectroscopy for on-site mycotoxin analysis. *Sci. Rep.* **2017**, *7*, 44028. [[CrossRef](#)]
40. Hossain, M.Z.; Goto, T. Near- and mid-infrared spectroscopy as efficient tools for detection of fungal and mycotoxin contamination in agricultural commodities. *World Mycotoxin J.* **2014**, *7*, 507–515. [[CrossRef](#)]
41. Li, F.L.; Xie, J.; Wang, S.; Wang, Y.; Xu, C.H. Direct qualitative and quantitative determination methodology for massive screening of DON in wheat flour based on multi-molecular infrared spectroscopy (MM-IR) with 2T-2DCOS. *Talanta* **2021**, *234*, 122653. [[CrossRef](#)]
42. Smeesters, L.; Meulebroeck, W.; Raeymaekers, S.; Thienpont, H. Non-destructive detection of mycotoxins in maize kernels using diffuse reflectance spectroscopy. *Food Control* **2016**, *70*, 48–57. [[CrossRef](#)]
43. Siuda, R.; Balcerowska, G.; Kupcewicz, B.; Lenc, L. A modified approach to evaluation of DON content in scab-damaged ground wheat by use of diffuse reflectance spectroscopy. *Food Anal. Methods* **2008**, *1*, 283–292. [[CrossRef](#)]
44. Tekle, S.; Bjørnstad, Å.; Skinnes, H.; Dong, Y.; Segtnan, V.H. Estimating Deoxynivalenol content of ground oats using VIS-NIR spectroscopy. *Cereal Chem.* **2013**, *90*, 181–185. [[CrossRef](#)]
45. De Girolamo, A.; Lippolis, V.; Nordkvist, E.; Visconti, A. Rapid and non-invasive analysis of deoxynivalenol in durum and common wheat by Fourier-Transform Near Infrared (FT-NIR) spectroscopy. *Food Addit. Contam. Part A* **2009**, *26*, 907–917. [[CrossRef](#)] [[PubMed](#)]
46. De Girolamo, A.; Cervellieri, S.; Visconti, A.; Pascale, M. Rapid analysis of Deoxynivalenol in durum wheat by FT-NIR Spectroscopy. *Toxins* **2014**, *6*, 3129–3143. [[PubMed](#)]
47. De Girolamo, A.; Cervellieri, S.; Cortese, M.; Porricelli, A.C.R.; Pascale, M.; Longobardi, F.; von Holst, C.; Ciaccheri, L.; Lippolis, V. Fourier transform near-infrared and mid-infrared spectroscopy as efficient tools for rapid screening of deoxynivalenol contamination in wheat bran. *J. Sci. Food Agric.* **2019**, *99*, 1946–1953. [[CrossRef](#)]
48. Kos, G.; Lohninger, H.; Krska, R. Fourier transform mid-infrared spectroscopy with attenuated total reflection (FT-IR/ATR) as a tool for the detection of *Fusarium* fungi on maize. *Vib. Spectrosc.* **2002**, *29*, 115–119. [[CrossRef](#)]
49. Öner, T.; Thiam, P.; Kos, G.; Krska, R.; Schwenker, F.; Mizaikoff, B. Machine learning algorithms for the automated classification of contaminated maize at regulatory limits via infrared attenuated total reflection spectroscopy. *World Mycotoxin J.* **2019**, *12*, 113–122. [[CrossRef](#)]
50. Horigome, J.; Kozuma, M.; Shirasaki, T. Fluorescence pattern analysis to assist food safety. *Hitachi Rev.* **2016**, *7*, 248–254.
51. Sikorska, E.; Khmelinskii, I.; Sikorski, M. Fluorescence spectroscopy and imaging instruments for food quality evaluation, Chapter 19. In *Evaluation Technologies for Food Quality*; Zhong, J., Wang, X., Eds.; Woodhead Publishing-Elsevier: Amsterdam, The Netherlands, 2019; pp. 491–533.

52. Fernandez-Romero, J.M.; Aguilar-Caballos, M.P. Fluorescence: Food Applications. In *Encyclopedia of Analytical Science*, 3rd ed.; Worsfold, P., Townshend, A., Poole, C., Eds.; Elsevier: Amsterdam, The Netherlands, 2018.
53. Fujita, K.; Tsuta, M.; Kokawa, M.; Sugiyama, J. Detection of Deoxynivalenol using fluorescence excitation-emission matrix. *Food Bioprocess Technol.* **2010**, *3*, 922–927. [[CrossRef](#)]
54. Fujita, K.; Tsuta, M.; Sugiyama, J.; Kushiro, M.; Shibata, M. Non-destructive measurement of Deoxynivalenol in wheat flour using fluorescence fingerprinting. *Nippon. Shokuhin Kagaku Kogaku Kaishi* **2011**, *58*, 375–381. [[CrossRef](#)]
55. Sugiyama, J.; Fujita, K.; Tsuta, M.; Kushiro, M. Detection of Deoxynivalenol in wheat flour using fluorescence fingerprint. *Procedia Food Sci.* **2011**, *11*, 1146–1151. [[CrossRef](#)]
56. Armenta, S.; Esteve-Turrillas, F.A.; Garrigues, S.; de la Guardia, M. *Green Approaches for Chemical Analysis*; Chapter 1; Gionfriddo, E., Ed.; Elsevier Inc.: Amsterdam, The Netherlands, 2023; pp. 1–37.
57. Pallone, J.A.L.; Caramês, E.T.D.S.; Alamar, P.D. Green analytical chemistry applied in food analysis: Alternative techniques. *Curr. Opin. Food Sci.* **2018**, *22*, 115–121. [[CrossRef](#)]
58. Armenta, S.; Garrigues, S.; de la Guardia, M. Green Analytical Chemistry. *TrAC Trends Anal. Chem.* **2008**, *27*, 497–511. [[CrossRef](#)]
59. Rasch, C.; Kumbé, M.; Löhmansröben, H.G. Sensing of mycotoxin producing fungi in the processing of grains. *Food Bioprocess Technol.* **2010**, *3*, 908–916. [[CrossRef](#)]
60. Bauriegel, E.; Herppich, W.B. Hyperspectral and chlorophyll fluorescence imaging for early detection of plant diseases, with special reference to fusarium spec. infections on wheat. *Agriculture* **2014**, *4*, 32–57. [[CrossRef](#)]
61. Jackson, J.E. *A User's Guide to Principal Components*; John Wiley & Sons Inc.: Hoboken, NJ, USA, 2003.
62. Mafata, M.; Brand, J.; Kidd, M.; Medvedovici, A.; Buica, A. Exploration of data fusion strategies using component analysis and multiple factor analysis principal. *Beverages* **2022**, *8*, 66. [[CrossRef](#)]
63. Liu, Z.; Forsyth, D.S.; Komorowski, J.P.; Hanasaki, K.; Kirubarajan, T. Survey: State of the Art in NDE data fusion techniques. *IEEE Trans. Instrum. Meas.* **2007**, *56*, 2435–2451. [[CrossRef](#)]
64. Tharwat, A. Linear vs. quadratic discriminant analysis classifier: A tutorial. *Int. J. Appl. Pattern Recognit.* **2016**, *3*, 145–180. [[CrossRef](#)]
65. Ballabio, D.; Todeschini, R. Multivariate Classification for Qualitative Analysis. In *Infrared Spectroscopy for Food Quality Analysis and Control*; Sun, D.W., Ed.; Elsevier Inc.: Amsterdam, The Netherlands, 2009; pp. 84–104.
66. Olivieri, P.; Downey, G. Multivariate class modeling for the verification of food-authenticity claims. *TrAC Trends Anal. Chem.* **2012**, *35*, 74–86. [[CrossRef](#)]

Disclaimer/Publisher's Note: The statements, opinions and data contained in all publications are solely those of the individual author(s) and contributor(s) and not of MDPI and/or the editor(s). MDPI and/or the editor(s) disclaim responsibility for any injury to people or property resulting from any ideas, methods, instructions or products referred to in the content.